Available online at www.sciencedirect.com

ScienceDirect

journal homepage: www.elsevier.com/locate/he

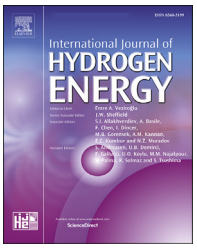

Potential of renewable surplus electricity for power-to-gas and geo-methanation in Switzerland

Martin Rüdisüli [a,*], *Robin Mutschler* [a], *Sinan L. Teske* [a], *Daniel Sidler* [b], *Daniela B. van den Heuvel* [c], *Larryn W. Diamond* [c], *Kristina Orehounig* [a], *Sven Eggimann* [a]

[a] *Urban Energy Systems Laboratory, Swiss Federal Laboratories for Materials Science and Technology, Empa, Dübendorf, Switzerland*

[b] *Energie 360° AG, Zurich, Switzerland*

[c] *Institute of Geological Sciences, University of Bern, Switzerland*

HIGHLIGHTS

- Run-of-river power plants are best suited to allocate geo-methanation.
- Industrial CO_2 is largely available and not constraining geo-methanation.
- An increase in load shifting power and capacity is required for power-to-gas.
- Transportation distanced between CO_2 sources and geo-methanation site are short.
- Geology constraints the potential of combining power-to-gas and geo-methanation.

ARTICLE INFO

Article history:
Received 14 September 2022
Received in revised form
5 December 2022
Accepted 24 December 2022
Available online xxx

Keywords:
Geo-methanation
CO_2 sources
Power-to-gas
PV
Run-of-river
Hydrogen

ABSTRACT

Energy systems are increasingly exposed to variable surplus electricity from renewable sources, particularly photovoltaics. This study estimates the potential to use surplus electricity for power-to-gas with geo-methanation for Switzerland by integrated energy system and power-to-gas modelling. Various CO_2 point sources are assessed concerning exploitable emissions for power-to-gas, which were found to be abundantly available such that 60 TWh surplus electricity could be converted to methane, which is the equivalent of the current annual Swiss natural gas demand. However, the maximum available surplus electricity is only 19 TWh even in a scenario with high photovoltaic expansion. Moreover, making this surplus electricity available for power-to-gas requires an ideal load shifting capacity of up to 10 times the currently installed pumped-hydro capacity. Considering also geological and economic boundary conditions for geo-methanation at run-of-river and municipal waste incinerator sites with nearby CO_2 sources reduces the exploitable surplus electricity from 19 to 2 TWh.

Abbreviations: DHW, domestic hot water; DSM, demand side management; CHP, combined heat and power; eqFLH, equivalent full load hours; MWIP, municipal waste incineration plant; PHS, pumped-hydro storage; PtG, power-to-gas; PtM, power-to-methane; PV, photovoltaic; RoR, run-of-river; SH, space heating; SMB, Swiss Molasse Basin; SNG, synthetic natural gas.

* *Corresponding author.*
E-mail address: martin.ruedisueli@empa.ch (M. Rüdisüli).

https://doi.org/10.1016/j.ijhydene.2022.12.290

Introduction

In many countries, including Switzerland, a large expansion of photovoltaic (PV) capacity is foreseen to meet climate protection targets [1,2]. This expansion is anticipated to happen along with a simultaneous phase-out of nuclear and fossil baseload electricity generation [3]. Because of the intermittent and stochastic nature of PV, the variability of electricity supply will increase and the importance of storage and flexibility will grow [4,5]. Demand side management (DSM) will help make use of more PV supply [6] during times of high PV generation in summer and at noon, however, PV generation may still be available in excess quantities even after shifting demand and supply to the same hours within an hourly to daily time scale [7]. Instead of curtailing this excess electricity, power-to-gas (PtG) can be employed to use renewable surplus electricity for producing hydrogen (H_2) and other gaseous energy carriers such as methane (CH_4). This allows for the storage of the generated gaseous energy carriers to overcome seasonal energy demand and supply discrepancies [8]. Sun and Harrison [9] showed that PtG using excess renewable electricity is also promising for hydrogen production from an economical point of view.

Power-to-methane

In the context of power-to-methane (PtM), hydrogen (H_2) along with carbon dioxide (CO_2) is converted to synthetic methane (CH_4) [10]. The methanation process (cf. Sabatier reaction [11]) can be achieved either catalytically or biologically. As power-to-methane takes as an input CO_2 from various sources (e.g. industry, thermal power plants, etc.), the release of CO_2 into the atmosphere is prevented. Power-to-methane is thus characterised by a closed carbon cycle. The benefits and potentials of power-to-methane have been assessed in several studies for different geographical contexts and different CO_2 sources [12–17]. Nielsen and Skov [18], for example, developed a spatial investment screening model for identifying PtM sites in Denmark. Reiter et al. [15], for the example of Austria, evaluated wind power plants and biogas upgrading facilities and found that they are well-suited CO_2 sources for PtM applications. For a German context, Schiebahn et al. [19] conducted a technological overview, systems analysis and economic assessment and found that PtM could only be realized at a global scale if it becomes economically competitive. Heymann et al. [20], moreover, showed by employing Composite Indicators that the economic viability of power-to-methane plants increases with their size and as projects move from research to pilot to commercial scale. Many studies point out that the most promising application of the produced synthetic methane can be found in the industrial and transportation sectors (Teske et al. [21], Kober et al. [22], Nazir et al. [23]).

Geo-methanation

Besides catalytic and biological methanation, which typically take place above ground, geo-methanation is a particular PtM path that allows for the conversion of hydrogen and CO_2 to synthetic methane with the help of methanogenic micro-organisms (archaea) in underground depth of more than 600 m [24].

To balance seasonal demand and supply discrepancies in a (future) energy system, the storage of large amounts of renewable energy becomes essential and is often the critical step, as storage is costly and influences the overall energetic efficiency of the system [25,26]. Geo-methanation combines storage and conversion of hydrogen, CO_2 and methane in a huge porous geological medium. In this way, synthetic (i.e. renewable) natural gas produced by geo-methanation can be directly stored underground within the same gas reservoir and retrieved whenever needed [27]. This possibility to combine conversion and storage of gaseous energy carriers underground has several advantages over conventional (i.e. above ground) catalytic and biological methanation:

i) As the underground provides huge naturally sealed porous formations with good gas mixing and flow capabilities as well as enormous pore volumes, a larger interface between the gaseous and aqueous phases can be established [28]. A potential analysis by Strobel et al. [26] shows a storage capacity of 850 Mio. m^3 in Germany, which could deliver renewable methane to over 600,000 households for heating.
ii) Since gas storage occurs underground, geo-methanation is generally not subject to safety issues such as fires, extreme weather conditions and sabotage or terrorist attacks [28].
iii) Costs are expected to become relatively low as operational and investment costs are lower than large-scale surface tanks. In particular, if geo-methanation can be combined with Carbon Capture and Storage/Utilization (CCS/U) it may become economically viable. In the "Underground Sun Conversion" project [29], the production costs of geo-methane in a CCU use case were estimated at 9–23 cent/kWh in 2025 and 10–20 cent/kWh in 2050. Thus, if electricity costs increase more than the investment costs of the plant and costs decrease due to learning effects, production costs will remain constant (or slightly increase) over time. Nonetheless, due to the large and highly site-specific influence of exploration and installation costs, a fair comparison of geo-methanation to conventional above ground methanation is still challenging and subject to further research [28].

So far, only a few studies have explored geo-methanation: While the review paper of Zivar et al. [30] looks at technical aspects and the feasibility of underground hydrogen storage in depleted hydrocarbon reservoirs, aquifers, and man-made underground cavities (caverns), Strobel et al. [26] explored the concept and potential of underground bio-methanation. Even more specifically, the "Underground Sun Storage" project [31] investigates technical, economical and legal issues of geo-methanation, while in its successor project "Underground Sun Conversion" [29], the actual biological geo-methanation process and its resilience were researched in detail.

Please cite this article as: Rüdisüli M et al., Potential of renewable surplus electricity for power-to-gas and geo-methanation in Switzerland, International Journal of Hydrogen Energy, https://doi.org/10.1016/j.ijhydene.2022.12.290

Integral assessment of power-to-gas and geo-methanation potential

Only a few exceptions (e.g. Ref. [32]) provide a combined assessment of PtG and geo-methanation for an entire country or a specific site. Such analysis is challenging as it requires integral modelling of a national energy system along with local characteristics of individual power plants and geological boundary conditions at a high spatial and temporal resolution [33]. Geological boundary conditions for geo-methanation include underground conditions suitable for microbiological activity (e.g. temperature), high enough permeability to allow injection/extraction and the existence of a cap rock layer to seal the produced methane underground [26,34]. Dopffel et al. [28] for instance showed that the chance of microbial activity is highest in aquifers and former gas reservoirs and lower for salt caverns. However, activities strongly depend on the specific local conditions.

To fully assess the potential of PtG and geo-methanation at a nationally aggregated scale and individual (optimal) sites, the availability of nearby industrial CO_2 and renewable surplus electricity must be known at the required spatio-temporal granularity. To be economically viable, two site options are ideal: either a large CO_2 source such as a cement plant or a renewable power plant such as a run-of-river hydropower plant [35]. Proximity to a CO_2 source has the advantage of saving CO_2 transportation and distribution costs. However, if no or only a limited amount of on-site electricity generation is available at the CO_2 source, additional electricity from the grid has to be used, which would incur additional costs in the form of grid fees. Therefore, PtG sites at power plants are generally more economically viable, particularly if CO_2 sources are nearby [80]. Municipal waste incineration plants (MWIP) feature both: sufficient on-site renewable electricity as well as large quantities of separable CO_2. Furthermore, run-of-river power plants are highly suitable as they generate large amounts of renewable electricity, particularly when surplus electricity from PV is largest (i.e. in summer).

Unique contribution and research questions

The overarching goal of this paper is to conduct a comprehensive investigation of the effective potential of PtG and geo-methanation at a national scale including specific sites located within areas of high geological potential for Switzerland. This investigation requires integrating a national electricity demand and supply model with corresponding data on the availability of CO_2 and geological conditions. To this end, a model framework is developed for Switzerland by combining a suite of different models that allow calculation of the potential methane yield via geo-methanation. Whereas potential CO_2 sources are well established from literature, their spatial identification for Switzerland and matching with the PtG potential and geo-methanation sites is novel. Introducing spatial constraints as well as techno-economic considerations is innovative and has so far been missing. To the best of the authors' knowledge, this study provides the first and most comprehensive assessment of this kind. While the focus is on Switzerland, methods and results may readily be applied and transferred to other countries.

Structure

The paper is structured as follows: In Section 2, the models employed including their base assumptions and input data are explained. Section 3 highlights the key results concerning the potential estimation of power-to-gas and geo-methanation in Switzerland. A conclusion and outlook based on the key findings are provided in Section 4. Additional information on data, methods and assumptions as well as accompanying results are provided in Supplementary Information (SI).

Methods

To assess the potential of PtG and geo-methanation, a modelling framework is set up by integrating a Swiss energy system model [36], a PtG model [21] and a 3D geological model [37]. In the energy system model of Rüdisüli et al. [36] future energy policy measures are added or subtracted at an hourly time scale from actual measurements and datasets from the electricity, heat and mobility sectors along with meteorological data and state-of-the-art technology specifications. Additionally, the PtG model of Teske et al. [21] is employed to estimate the spatio-temporal availability of net surplus electricity, industrial CO_2 point sources and boundary conditions of the Swiss natural gas infrastructure. Finally, the 3D geological model GeoMol provides information on deep underground rock types and their distribution, temperature isotherms, and fold and fault structures in the Swiss Molasse Basin (SMB).

A graphical overview of the modelling framework is provided in Fig. 1. Hourly profiles of the Swiss electricity demand and supply are created for four energy system transition scenarios based on existing national and international studies, namely the Swiss "Energy Perspective 2050+" (EP2050+) [1] and the European "Ten Year Network Development Plan 2018" (TYNDP) [2]. Hourly hydropower supply is adjusted based on a heuristic re-allocation approach and ideal load shifting is applied. This yields a daily net surplus electricity amount that can be converted to hydrogen (H_2) via water electrolysis at run-of-river (RoR) and/or municipal waste incineration plants. Along with CO_2 from industrial point sources, namely cement (CEM), municipal waste incineration (MWIP) and wastewater treatment plants (WWTP), hydrogen is converted to methane (CH_4) via geo-methanation. The produced CH_4 is eventually fed into the natural gas grid to meet the daily demand for natural gas. In the following sections and in the SI, all of these steps and inputs are described in more detail.

Flexibility and net surplus electricity

For PtG and geo-methanation, the availability of renewable surplus electricity is crucial [21]. Electricity surpluses occur if the momentary electricity supply is larger than the momentary electricity demand (and vice versa for deficits). To obtain these surpluses and derive daily net surpluses, the Swiss electricity system is modelled based on hourly demand and supply profiles (see Sections 2.3–2.4). The net surpluses are defined as the share of the total surpluses that remains after

Please cite this article as: Rüdisüli M et al., Potential of renewable surplus electricity for power-to-gas and geo-methanation in Switzerland, International Journal of Hydrogen Energy, https://doi.org/10.1016/j.ijhydene.2022.12.290

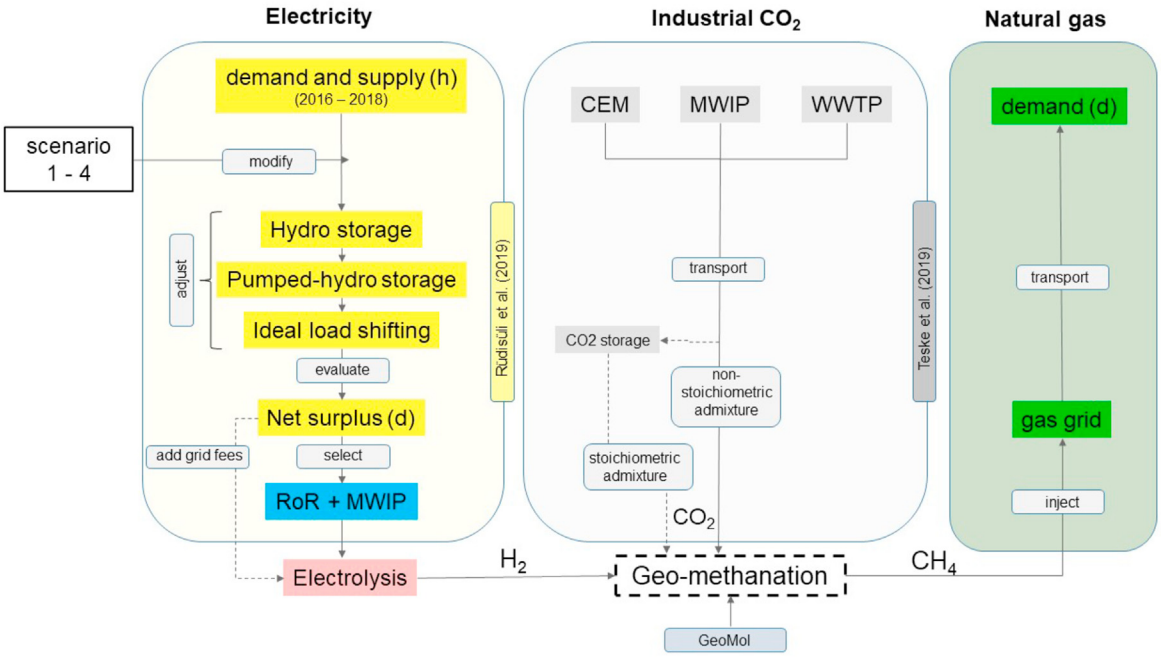

Fig. 1 – Schematic overview of the steps and inputs employed to derive renewable CH_4 via power-to-gas and geo-methanation from industrial CO_2 and renewable H_2. Scenarios 1–4 are based on the Swiss energy system's transition towards net-zero by 2050 according to the "Energy Perspective 2050+" (EP2050+) [1].

ideal load shifting (i.e. without losses) within 24 h to avoid curtailment of renewable surplus electricity. This load shifting can be achieved by short-term electricity storage technologies such as batteries, flexible hydropower (see Section 2.5.5) or demand side management (DSM) such as charging electric vehicles at noon instead of during evening and night hours. The dark green area in Fig. 2 illustrates the shifted surplus of electricity at noon to offset night deficits within 24 h. The light green area illustrates the remaining net surplus electricity, which can then be used for PtG and geo-methanation. Corresponding net surplus electricity is evaluated at the national scale and for individual sites.

Case study context

Case study input data

Fig. 3 shows a map of Switzerland with all its 577 RoR power plants and 30 municipal waste incineration plants (MWIP), all considered industrial CO_2 sources (30 MWIP, 6 CEM, 759 WWTP) and the Swiss natural gas grid. Of the 19,300 km long natural gas grid, 2,300 km belong to the high pressure (5–85 bar) and 17,000 km to the local low-pressure distribution grids (0.02–5 bar) [38].

From a geological point of view, the Swiss Molasse Basin (SMB) is the main area of interest for geo-methanation. Several potential reservoir formations (e.g. sandstones) sealed by caprocks (e.g. clay stones) suitable for gas injection have been identified previously [39]. The Alps and the Jura Mountains were deemed unsuitable for geo-methanation due to less permeable rock formations and a high abundance of faults and fractures, resulting in poor reservoir characteristics. A geological 3D model (GeoMol) [40] is available for the SMB and adjacent Jura Mountains (lighter area in Fig. 3). Within this perimeter, an underground temperature model has been established (darker area). This inner geological perimeter forms the basis of the geological appraisal of the suitability of the SMB for geo-methanation [34]. No geological assessment of areas outside the inner perimeter is currently available. However, the geology may still be suitable for geo-methanation in these areas [34].

Swiss energy system scenarios

The potential of PtG and geo-methanation is evaluated within four distinct Swiss energy system transition scenarios: While scenario 1 serves as the reference for the current Swiss energy system, scenarios 2–4 represent future energy system configurations with increasing substitution of nuclear power by renewable energies and increasing electrification of heat and mobility. Renewable energy expansion is primarily achieved by PV. These scenarios do not represent specific future years but represent snapshots of important intermediate states of the Swiss energy transition towards net zero. The scenarios can roughly be allocated to the years 2020, 2030, 2040 and 2050, according to the official transition pathway given by scenario ZERO-BASIS of EP2050+ [1]. All four scenarios are grounded on the three historical years 2016, 2017 and 2018 concerning load and climate profiles. Using three years allows capture of the variability due to different weather conditions and approximate potential climate change impacts, as these three years already contain characteristics of a future climate with mild and wet winters as well as hot and dry summers [41]. Further impacts of climate change on energy demands such as from additional cooling or shifted hydropower are not considered.

Please cite this article as: Rüdisüli M et al., Potential of renewable surplus electricity for power-to-gas and geo-methanation in Switzerland, International Journal of Hydrogen Energy, https://doi.org/10.1016/j.ijhydene.2022.12.290

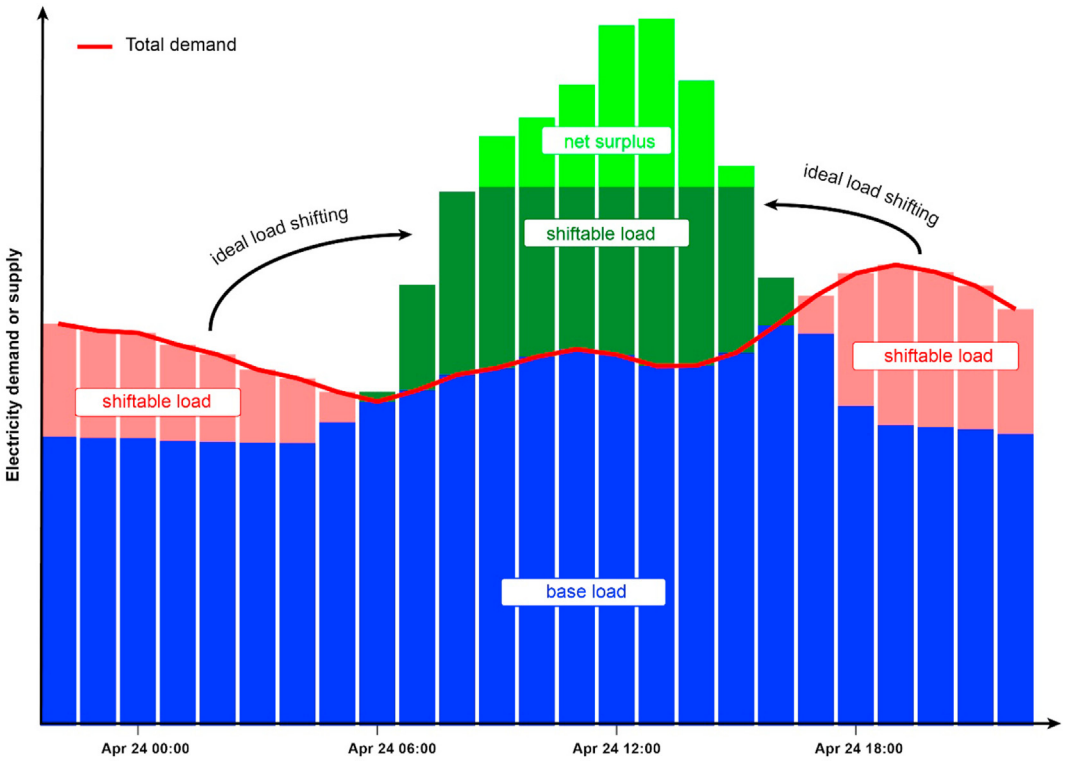

Fig. 2 – Concept of ideal load shifting to offset day and night discrepancies between electricity demand and supply within 24 h (adapted from Teske et al. [35]). Ideal load shifting denotes the absence of losses and physical limitations.

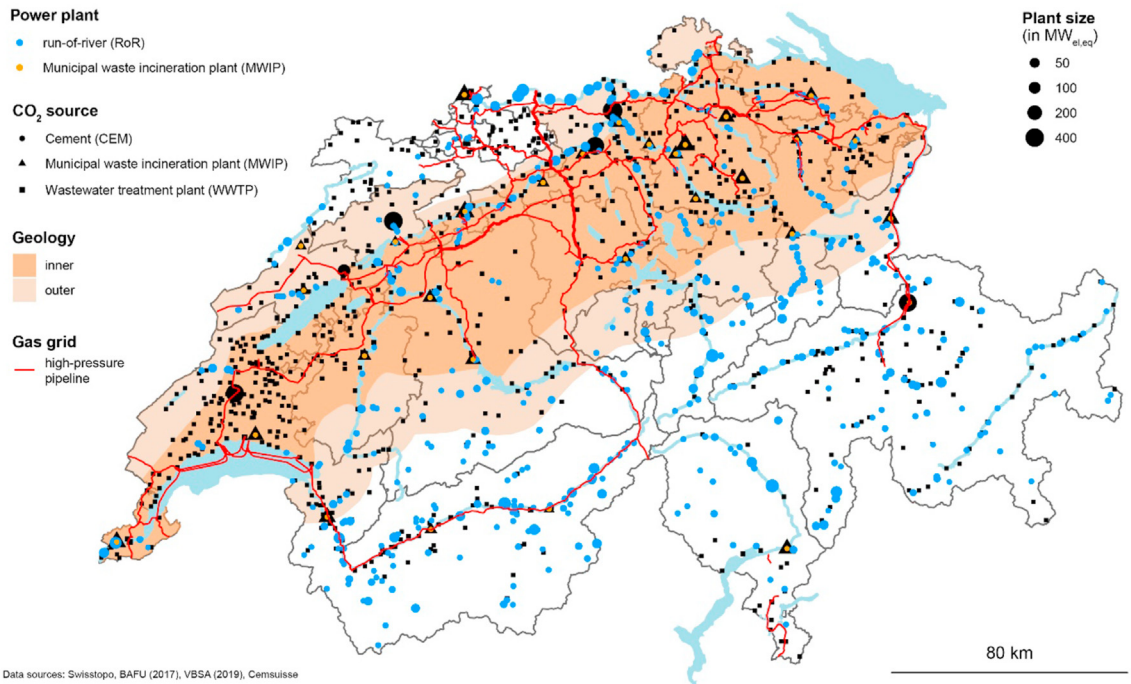

Fig. 3 – Overview of all RoR hydropower plants, industrial CO_2 sources and the high-pressure Swiss natural gas grid. In addition, the coverage of the geological model (outer) plus subsurface temperature model (inner perimeter) is shown. In the non-shaded areas, geo-methanation is likely unsuitable due to geological limitations.

Please cite this article as: Rüdisüli M et al., Potential of renewable surplus electricity for power-to-gas and geo-methanation in Switzerland, International Journal of Hydrogen Energy, https://doi.org/10.1016/j.ijhydene.2022.12.290

Demand modelling and data preparation

Space heating and domestic hot water

The current annual weather-adjusted Swiss space heating (SH) and domestic hot water (DHW) energy demand is about 72 TWh and 12 TWh, respectively [42]. While for SH a substantial demand reduction is anticipated by retrofitting and renewal of buildings, no absolute reduction is assumed for DHW. The evolution of both heating demands in the four scenarios is in line with scenario ZERO-BASIS of EP2050+ [1] and summarized in SI Table 1. SH and DHW are currently primarily covered by fossil energy carriers such as heating oil and natural gas.

Gas

Biomethane is produced almost uniformly and throughout the year both in Switzerland and the European Union. Synthetic natural gas (SNG) is produced via PtG, whenever there is renewable net surplus electricity available. The total gas demand of Switzerland is currently about 34 TWh (scenario 1), which is mainly met by imported fossil natural gas [43]. To decarbonise the energy system, SNG must only be physically imported in case gas demand exceeds the availability of domestic renewable gases. Future gas demand is assumed to arise primarily from industry and energy conversion to process heat and combined-heat-and-power (CHP). For instance, industries that are hard to electrify would still rely on methane, particularly high-temperature processes, in which constant gas demand is assumed throughout the year. For transportation, future short-distance and passenger vehicles are assumed mostly to be electrified, whereas heavy-duty and long-distance vehicles (e.g. trucks and buses) rely more on gaseous energy carriers such as H_2 and SNG.

Demand for low-temperature heating constitutes the remaining (and declining) share of the future gas demand. We assume that on a district level, gas-fired CHP plants will still provide (at least temporarily) electricity and heat, particularly in winter. This gas demand follows a distinct seasonal pattern with a peak in January and virtually no demand in summer (i.e. July). Table SI 2 summarises the evolution of the gas demand in all four scenarios for the energy sectors industry, transportation and others. This demand evolution is in line with scenario ZERO BASIS of EP2050+ [1]. The monthly disaggregation of gas demand by the different energy sectors is illustrated in Figure SI 1. Based on the future annual gas demand per sector, the seasonal demand patterns are modelled according to the normalized daily demand of gas customers, which are extrapolated from historical data on the Swiss gas market.

Electricity

A summary of the main boundary conditions and assumptions of the annual electricity demand in the four scenarios is provided in Table SI 3. The total electricity demand increases from currently about 60 TWh (reference scenario 1) to about 67 TWh in scenario 4. The individual demand components are derived as follows.

- *Base electricity demand (including electricity savings)*: Base electricity demand comprises all end-use electricity consumed in Switzerland, including transmission and transformation losses of about 6% [44]. The annual base electricity demand is calculated from the 2016 to 2018 end-use electricity demand profiles at a 15-min resolution from the Swiss transmission system operator (TSO) Swissgrid [45] and aggregated to an hourly time scale. The future base electricity demand (without the additional electricity demand from heating and transportation) is based on reduction paths in scenario ZERO-BASIS in EP2050+ [1], which also account for projected population and economic (i.e. GDP) growth. Base electricity demand reduction is mainly achieved by sufficiency and efficiency measures (e.g. more efficient lighting and appliances, etc.). The defined reductions in the future scenarios 2–4 are linearly applied to the reference hourly electricity demand profiles of 2016–2018 (i.e. scenario 1). This allows daytime- and weather-dependent electricity demand variations to be neglected.
- *E-mobility*: Annual electricity demand of battery electric vehicles (BEV) is taken from scenario ZERO-BASIS of EP2050+ [1], which assumes net-zero greenhouse gas emissions in Switzerland in 2050 by fully replacing internal combustion engine vehicles with BEV. For efficiency and cost reasons, electricity-based synthetic fuels (e.g. SNG) are not considered and only a small market share of H_2 for fuel cell electric vehicles is assumed. Detailed modelling of the future car fleet yields a total additional BEV electricity demand of 11 TWh in 2050. More information is provided in SI Section 1.2.
- *Heat pumps for SH and DHW*: In scenario 4, 75% of the annual SH demand is provided by heat pumps as derived in Rüdisüli et al. [36]. This percentage is linearly adjusted in the other future scenarios (2 and 3) based on an assumed more progressive expansion of heat pumps compared to EP2050+ [1]. The exact procedure applied to obtain the hourly heat pump electricity demand profiles is outlined in SI Section 1.3. Current hourly electricity demand for DHW mainly stemming from resistive water heaters is assumed to remain constant because of the increased substitution of fossil water boilers by heat pumps.

Supply modelling and data preparation

The total electricity supply increases from about 61 TWh in reference scenario 1 to about 76 TWh (+25%) in scenario 4. Table SI 4 summarises the main boundary conditions and assumptions on annual electricity supply for all scenarios. In the following, the derivation of each part of the electricity supply mix is described in more detail.

Nuclear

The annual generation of nuclear power in the four scenarios is based on different phase-out assumptions: In scenario 1, all Swiss nuclear power plants (including Mühleberg, which was shut down in 2019) are still operational. In scenario 2, only the largest Swiss nuclear power plant Leibstadt (1.3 GW) is still operational, all other nuclear power plants are phased out after an assumed lifetime of 50 years. A constant generation profile of Leibstadt is used, having only a 30-day planned outage due to annual revisions in June. Complete phase-out of all nuclear power plants is assumed in scenarios 3 and 4. The

Please cite this article as: Rüdisüli M et al., Potential of renewable surplus electricity for power-to-gas and geo-methanation in Switzerland, International Journal of Hydrogen Energy, https://doi.org/10.1016/j.ijhydene.2022.12.290

hourly generation profile for 2016 to 2018 is adopted from ENTSOE's transparency platform [46].

Wind

For scenario 1, historical annual wind generation from 2016 to 2018 is used [47]. For scenarios 2 to 4, the annual wind generation is adopted from EP2050+ [1]. The wind generation profile is generated from hourly capacity factors of current onshore Swiss wind turbines from renewables.ninja [48]. These capacity factors are linearly scaled to the annual wind generation in each scenario.

Photovoltaics

In scenario 1, the annual PV generation corresponds to the historical values from 2016 to 2018 [47]. In scenarios 2 and 3, the annual PV generation is equivalent to the phased-out nuclear power, while in scenario 4, PV generation also covers the additional electricity demand from heat and mobility. Hourly PV generation profiles are estimated based on the methodology described in Walch et al. [49] and applied to irradiance data from MeteoSchweiz [50]. All roofs with tilt angles below 10° are defined as flat roofs, for which panels are modelled as alternating east and west-facing rows at 15° tilt. The obtained hourly PV generation profiles of individual roofs are aggregated at the national scale by selecting the roofs with the highest annual yield first. This allows implementation of a strategic PV expansion by reaching the predefined annual generation in the scenarios with the least number of roofs [51].

Combined-cycle gas turbine

In all scenarios, it is assumed that no new domestic combined cycle gas turbine (CCGT) power plants are built or used, as this would not comply with current Swiss greenhouse gas mitigation targets.

Waste-to-energy

Waste-to-Energy refers to electricity produced at the 30 Swiss MWIP. The total annual electricity generation of all MWIP (cf. Section 2.5) is assumed to be constant at 2.1 TWh per year, which is in line with official statistics [52]. For future scenarios, this waste-to-energy electricity generation is assumed to remain constant. Regarding the hourly generation, a constant generation of 240 MW_{el} is assumed, irrespective of seasonally varying waste incineration schedules.

Hydropower

According to the Swiss national hydropower statistics [53], 577 RoR units with a power larger than 0.3 MW_{el} were available in 2018 to produce about 16 TWh of renewable electricity. This generation is assumed to remain constant in all scenarios. No additional capacity extension is assumed due to limited expansion potential [1]. SI Section 1.4 provides a detailed overview of all Swiss RoR hydropower plants with an installed capacity of more than 25 MW_{el}. Hourly generation profiles are adopted using the method described in SI Section 1.4.

Storage hydropower plants (HYD_DAM) are able to shift their generation (within certain limits) to times of high electricity demand (i.e. prices). As a proxy for electricity prices, the residual load is used [54,55]. The residual load is the momentary difference between the electricity demand and all inflexible (i.e. must-run) electricity generation (i.e., PV, wind, run-of-river, nuclear and waste-to-energy). The residual load is positive for hours with deficits (i.e. demand larger than supply) and negative for hours with surpluses (i.e. supply larger than demand). Especially in summer, also HYD_DAM is partially forced to constantly produce electricity due to high natural inflows and limited storage capacities in smaller retention reservoirs. This inflexible share of HYD_DAM is heuristically modelled according to Beer [56] (see SI Section 1.5).

For pumped-hydro storage (PHS), flexible pumping is implemented within five consecutive days as an additional electricity demand. An updated residual load profile including the modelled HYD_DAM generation is used and inverted such that the hours with the largest surplus (e.g. lowest prices) are prioritized for pumping, and hours with the highest deficits (e.g. highest prices) are used for turbination such that a maximum price spread (arbitrage) can be achieved. As a boundary condition for PHS, pumping can only happen in surplus hours, while turbining can only happen in deficit hours. Moreover, the maximum pumping and turbination power of 3.7 GW must not be exceeded and the maximum storable electricity within five consecutive days is determined a priori as either the total Swiss PHS storage capacity of 300 GWh [57] or the minimum of the summed surpluses and deficits within five consecutive days. A general round-trip efficiency of 80% is assumed.

CO_2 modelling data preparation

CO_2 is a prerequisite for the conversion of H_2 to CH_4 via geo-methanation. The CO_2 is separated and supplied in concentrated form from industrial CO_2 point sources. Due to well-established CO_2 separation technologies and market maturity, the only CO_2 sources considered are cement plants (CEM), municipal waste incineration plants (MWIP) and wastewater treatment plants (WWTP) (see Sections 2.5.1–2.5.3). CO_2 emissions from (petro-)chemical and metallurgical industries are ignored, as their CO_2 emissions, albeit of considerable quantitative relevance [58,59], are typically strongly process-dependent and therefore hard to exploit. Direct air capture is not considered either, since exploiting CO_2 from point sources poses an economic advantage over direct air capture, where CO_2 is only available in small concentrations (about 420 ppm) [60] and therefore more expensive to separate [61].

Cement plants (CEM)

Currently, there are 6 cement plants (CEM) in Switzerland [62] from which CO_2 is emitted into the atmosphere in the exhaust air stream. One-third of this CO_2 stems from the combustion process to supply heat to the rotary kiln, while the remaining two-thirds of CO_2 are geogenic and stem from the conversion of clinker ($CaCO_3$) to calcium oxide (CaO) [63]. The volumetric CO_2 content in the exhaust is approximately 14–35% [64] and inexpensive separation is possible during flue gas cleaning by amine scrubbing. The relevant CO_2 emissions are determined from the cement volumes published by the cement plants using an emission factor of 0.59 t CO_2 per tonne of cement [65].

Please cite this article as: Rüdisüli M et al., Potential of renewable surplus electricity for power-to-gas and geo-methanation in Switzerland, International Journal of Hydrogen Energy, https://doi.org/10.1016/j.ijhydene.2022.12.290

Municipal waste incineration plants (MWIP)

The 30 MWIP in Switzerland [66] emit CO_2 as a product of their combustion process. About half of this CO_2 stems from fossil fuel-based waste (e.g., plastic) [67] while the other half is biogenic (food, wood, etc.) and therefore CO_2 neutral [68]. With a volumetric fraction of about 10% CO_2 in the exhaust fumes [69,70], inexpensive CO_2 separation is possible, as with CEM, as part of flue gas cleaning using amine scrubbing. To estimate CO_2 amounts from MWIP, the annual amount of combustible waste published by the MWIP on their websites is multiplied by an emission factor of 1.06 t CO_2 per tonne of waste [71].

Wastewater treatment plants (WWTP)

CO_2 emissions from WWTP result from anaerobic sludge digestion (fermentation), in which CO_2, together with CH_4, is the main constituent of sewage gas [72]. The volumetric fraction of CO_2 is about 33% and of nearly 100% biogenic origin. Sewage gas is typically either already treated and fed into the natural gas grid, flared or used in on-site CHP plants for the WWTP's electricity and heat demand [73]. Unlike CEM and MWIP, using CO_2 from WWTP has the advantage that no additional CO_2 separation and gas upgrading are needed [74]. Instead, CO_2 can be used directly for PtG along with H_2 [74].

In the year 2017, the reported number of Swiss WWTP with a dimensioning size of more than 200 population equivalents (pe) was 759 [75]. For economic and operational reasons, only larger WWTP (pe > 10,000) are considered. Small-scale and special industrial WWTP or plants without anaerobic sludge digestion are neglected. The CO_2 emission factor of 10 kg_{CO2}/(pe * year) is derived from reported quantities of sewage gas and population equivalents from the Swiss Canton of St. Gallen [76].

CO_2 availability, requirements and separation

In this study, constant CO_2 emissions are assumed throughout the year, which is generally true for these CO_2 point sources. Under realistic conditions, only about 75%–90% of the CO_2 in the exhaust fumes of CEM and MWIP can technically be separated by amine scrubbing [64]. At WWTP, CO_2 from sewage can be used for PtG without additional CO_2 separation and upgrading [74]. Therefore, a conservative separation efficiency of 75% is assumed for CEM and MWIP and 100% for WWTP.

For stoichiometric conversion of H_2 and CO_2 to CH_4 according to Sabatier's reaction ($4H_2 + CO_2 = CH_4 + 2H_2O$), 5.5 g_{CO2} per g_{H2} are needed under standard conditions (molar mass of $CO_2 = 44$ g and of $H_2 = 2$ g). With a lower heating value of 33.3 kWh/kg_{H2}, 166 t CO_2 are needed per GWh_{H2}. Assuming a 57% efficient electrolysis [21], 94.1 t CO_2 are needed per GWh of (surplus) electricity.

A summary of the individual plant and cumulative CO_2 emissions is provided in SI Section 1.6.

CO_2 and CH_4 transportation

No CO_2 transportation is needed for PtG at MWIP, as the PtG plant location is assumed to be on the corresponding premises. For PtG at RoR sites, transportation of CO_2 by truck or pipeline is generally required. To find nearby CO_2 sources for each RoR power plant, an underlying transportation problem is solved with the help of the R package lpSolve and its function lp.transport [77]. The cost of CO_2 transportation from its source (i) to its sink (j) at the RoR plants is approximated by:

$$cost_{ij} = \frac{\text{distance}_{ij}}{\min(CO_2\text{available}_i, CO_2\text{needed}_j)} \quad (1)$$

where distance_{ij} is the Euclidean distance between two locations i and j, while $CO_2\text{available}_i$ is the total annual CO_2 available at source i and $CO_2\text{needed}_j$ is the CO_2 needed annually for full conversion of all available net surplus electricity to H_2 at RoR site j, assuming a conversion factor of 94.1 t CO_2/GWh_{el}. Besides the transportation distance, the employed cost function accounts for both required and available CO_2. This favours a small number of large CO_2 sources instead of several adjacent smaller ones. Neither geographical nor logistical transportation limitations are considered. Transportation of CH_4 is assumed to have negligible losses and CH_4 injection into the existing natural gas grid is assumed at no additional cost. Although gas is preferably injected into the high-pressure grid at particular gate and customs stations, detailed cost simulation is challenging as costs are highly dependent on the typically unknown reservoir pressures, etc.

Results and discussion

Dispatch of flexible hydropower

In Fig. 4a–c the dispatch of flexible hydropower (PHS and storage) in winter, spring and summer is shown according to the outlined heuristic model described in Section 2.4.6. In all seasons, flexible hydropower (Dam flex.) is gradually shifted away from noon hours, when PV is dominant (and prices are low), towards evening and night hours, when supply deficits (and therefore prices) increase due to additional BEV charging and declining nuclear supply. With PHS, inexpensive surplus electricity at noon is pumped and shifted towards more profitable evening and night hours. In winter (see Fig. 4a), not enough surplus electricity is available to cover these night deficits, particularly in scenarios 1 and 2. In scenarios 3 and 4, due to a large PV expansion of 25 TWh and 35 TWh, respectively, surplus electricity becomes available even in winter (at noon). During the intermediate season (Fig. 4b), there is often enough surplus electricity available at noon to completely cover evening and night deficits, particularly in scenarios 2, 3 and 4. However, due to limited installed PHS capacities (i.e., 3.7 GW), some deficits cannot be offset, although enough surplus electricity would be available at noon. In summer (Fig. 4c), all scenarios show surplus electricity almost throughout the day. The reason is that flexible hydro storage capacities, although shifted away from noon hours, are still available in excess. This situation, which would result in the curtailment of renewable energy, can only be avoided by a different (i.e. less economically driven) seasonal dispatch strategy of flexible hydropower or other means of seasonal storage such as PtG and geo-methanation.

Simulated flexibility for ideal load shifting

The required daily amount of flexibility (in GWh) for ideal load shifting is shown in Fig. 5. While little additional

Please cite this article as: Rüdisüli M et al., Potential of renewable surplus electricity for power-to-gas and geo-methanation in Switzerland, International Journal of Hydrogen Energy, https://doi.org/10.1016/j.ijhydene.2022.12.290

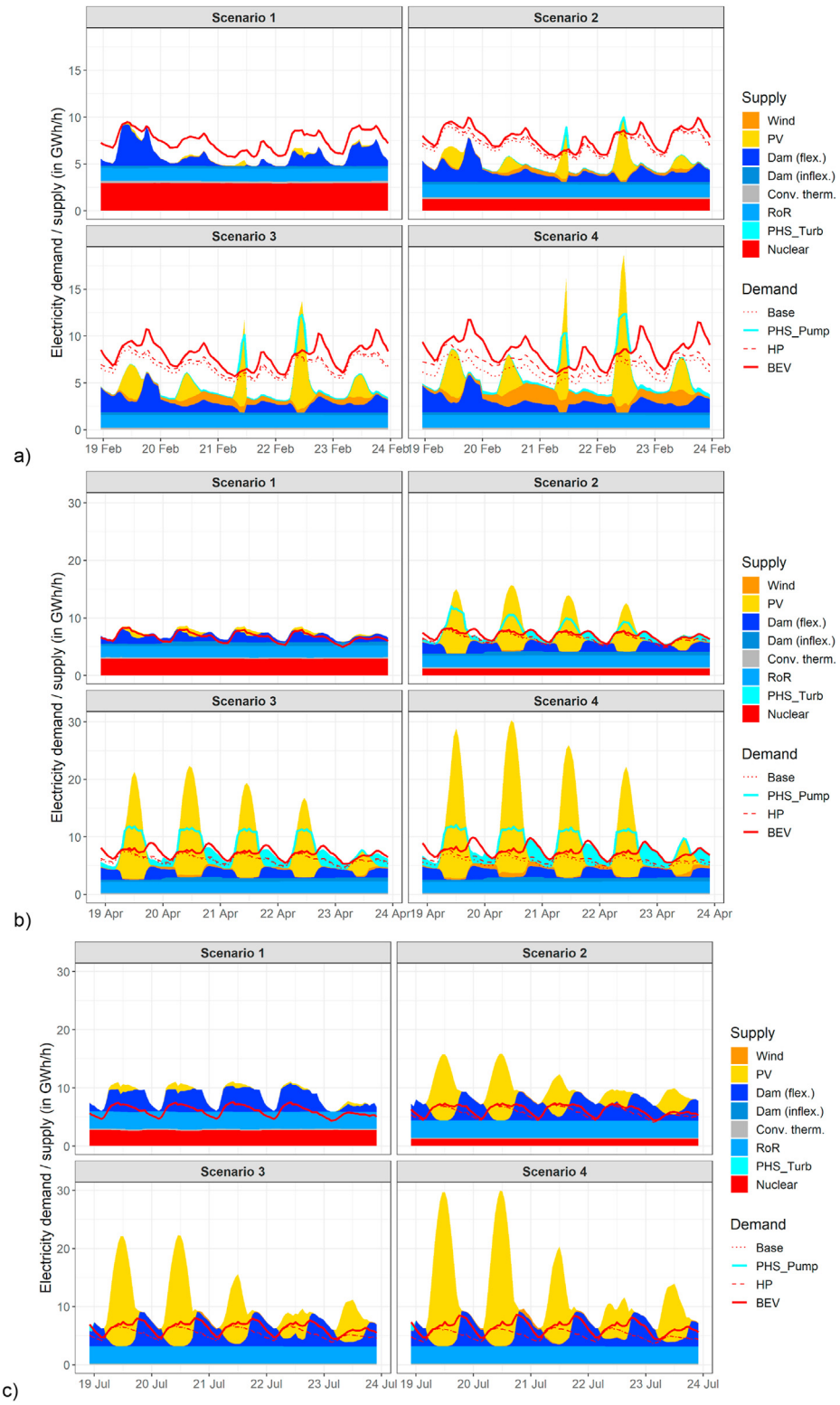

Fig. 4 – Hourly demand (lines) and supply (areas) of electricity including the dispatch of flexible hydropower (Dam and PHS) and inflexible supply (Wind, PV, RoR, Conv. therm, Nuclear) for an exemplary five consecutive days in all scenarios in a) winter b) spring and c) summer.

Please cite this article as: Rüdisüli M et al., Potential of renewable surplus electricity for power-to-gas and geo-methanation in Switzerland, International Journal of Hydrogen Energy, https://doi.org/10.1016/j.ijhydene.2022.12.290

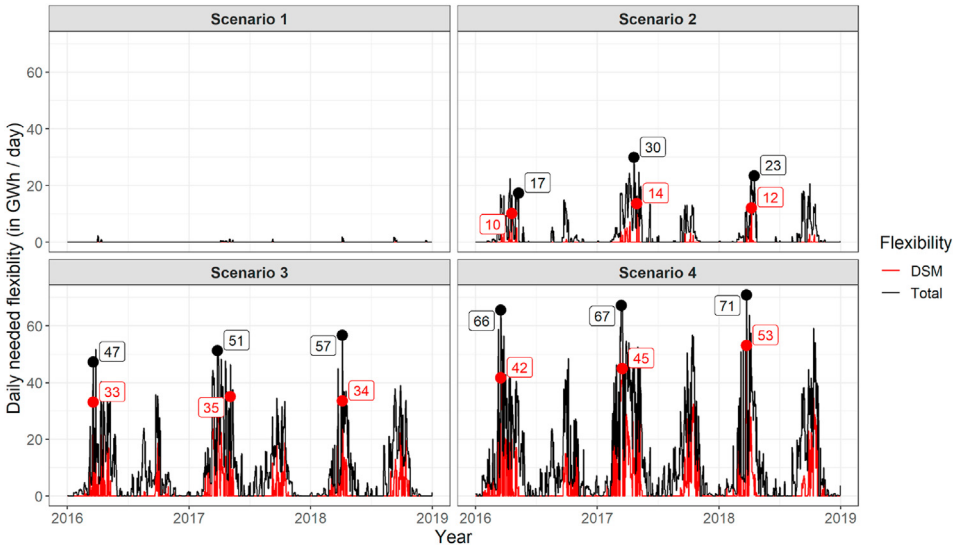

Fig. 5 – Daily flexibility (in GWh per day) needed to offset daily deficits by ideal load shifting. "Total" flexibility includes also the flexibility of existing pumped-hydro storage (PHS), while "Demand Side Management" (DSM) only looks at the additionally needed flexibility (i.e. in addition to the existing PHS). Labelled dots display annual maxima.

flexibility is needed in scenario 1, flexibility needs gradually increase to a maximum of 53 GWh/day in Scenario 4 in the 2018 weather year. A maximum combined flexibility of about 70 GWh/day is required in scenario 4 considering all flexibility, including the one from available pumped-hydro storage (PHS).

Daily peak power (i.e., maximum in each day) needed for ideal load shifting is high, as shown in Fig. 6 both in chronological and descending order. In scenario 4, the maximum daily required peak power exceeds 25 GW, typically at noon when PV generation is maximal. In scenario 3, a peak power of up to 18 GW is still needed. In all situations, the installed PHS pumping power of 3.7 GW is already exploited (subtracted).

This illustrates that the requirements for ideal load shifting are high concerning the needed power. The steep slope of the ordered (orange) representation shows that peak power is needed only during a few particular hours of the year and curtailing these peaks (e.g. at 20 GW) would not result in an excessive spill of electricity, yet make load shifting more economically viable [21].

Available net surplus electricity

The available annual net surplus electricity for PtG after ideal load shifting is displayed in Fig. 7 in dark green. For comparison, also the corresponding net deficits (black), and the gross

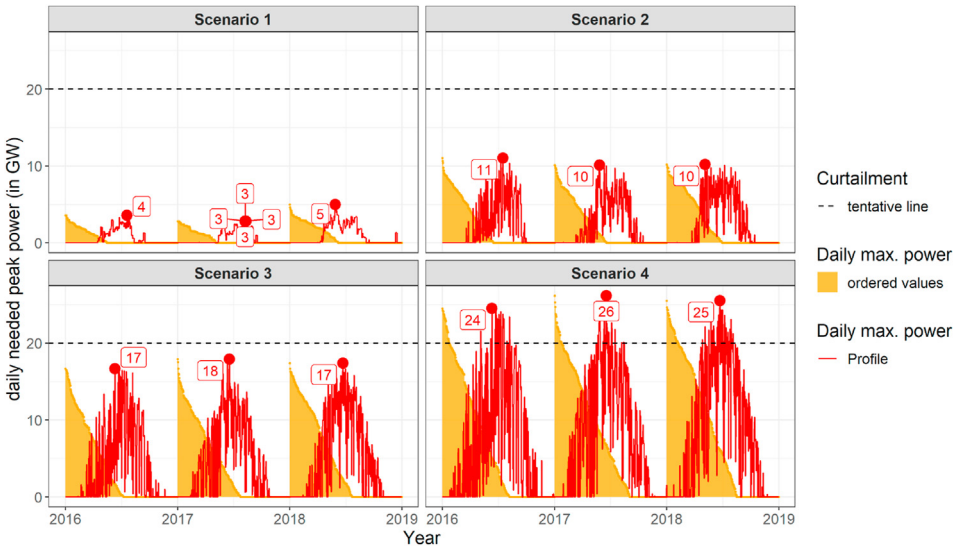

Fig. 6 – Daily peak power (in GW) needed for ideal load shifting sorted in chronological (red lines) and descending (orange area) order. The annual maximum (in summer) is indicated by a labelled red dot. (For interpretation of the references to colour in this figure legend, the reader is referred to the Web version of this article.)

Please cite this article as: Rüdisüli M et al., Potential of renewable surplus electricity for power-to-gas and geo-methanation in Switzerland, International Journal of Hydrogen Energy, https://doi.org/10.1016/j.ijhydene.2022.12.290

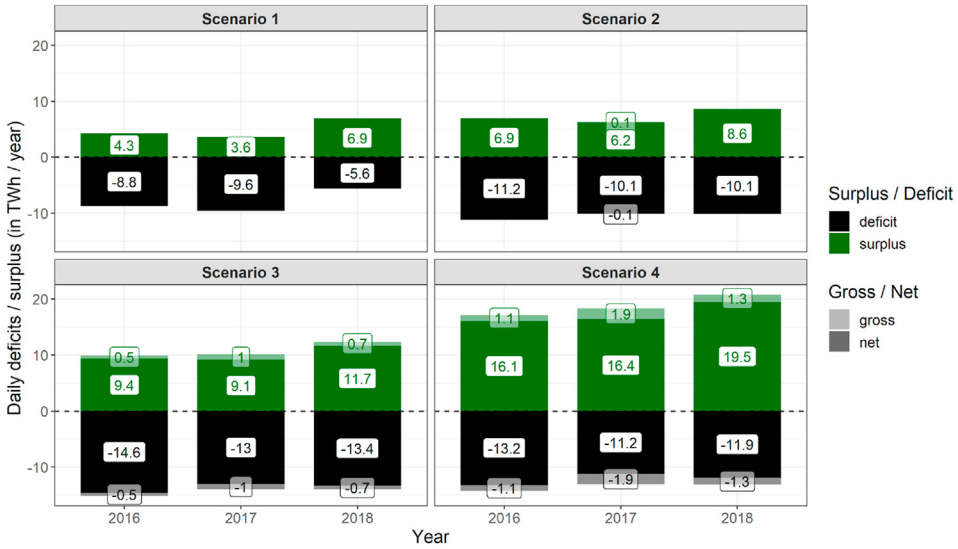

Fig. 7 – Annual net (dark green and black) and gross (light green and grey) electricity surpluses (positive values) and deficits (negative values) in each scenario. (For interpretation of the references to colour in this figure legend, the reader is referred to the Web version of this article.)

deficits (grey) and gross surpluses (light green), are displayed. Gross deficits and surpluses occur before ideal load shifting has been applied. Annual net surpluses range between 3.6 TWh (scenario 1) and 19.5 TWh (scenario 4). As exports are not allowed in this study, the effectively useable net surplus for PtG would need to be reduced by such an export, particularly in scenario 1. Exports would however gradually diminish in scenarios 2–4 due to similar surplus situations in neighbouring countries [78]. In all scenarios, the difference between net and gross surplus or deficits is comparatively negligable, hence only a relatively small amount of daily surpluses or deficits can be offset by ideal load shifting, while the largest shares of net surpluses or deficits feature a seasonal pattern that can only be offset by seasonal storage such as PtG and geo-methanation.

Exploitable net surplus electricity

The daily amount of net surplus electricity available in Switzerland is shown in Fig. 8. The share of simultaneously exploitable PtG at all MWIP (orange), all RoR power plants (blue) and both plant types combined (yellow) is also shown. While in scenarios 1 and 2 almost 100% of the net surplus (5–7 TWh) can be exploited at MWIP and RoR power plants, this share decreases substantially in the two other scenarios. In scenario 4, having the highest degree of PV penetration and

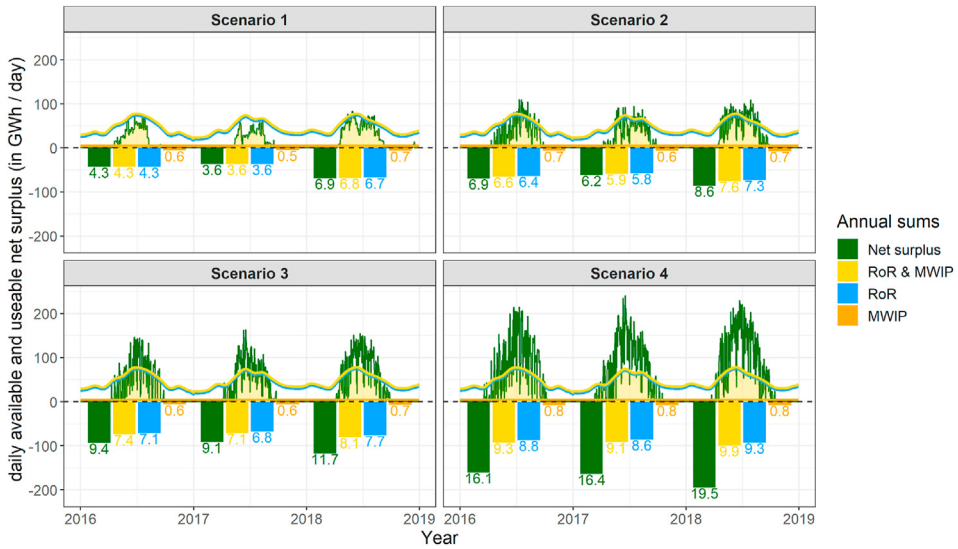

Fig. 8 – Daily (line) and annually (bars) available (green) and exploitable (yellow, blue and orange) net surplus electricity at RoR plants, MWIP and combined, respectively. (For interpretation of the references to colour in this figure legend, the reader is referred to the Web version of this article.)

Please cite this article as: Rüdisüli M et al., Potential of renewable surplus electricity for power-to-gas and geo-methanation in Switzerland, International Journal of Hydrogen Energy, https://doi.org/10.1016/j.ijhydene.2022.12.290

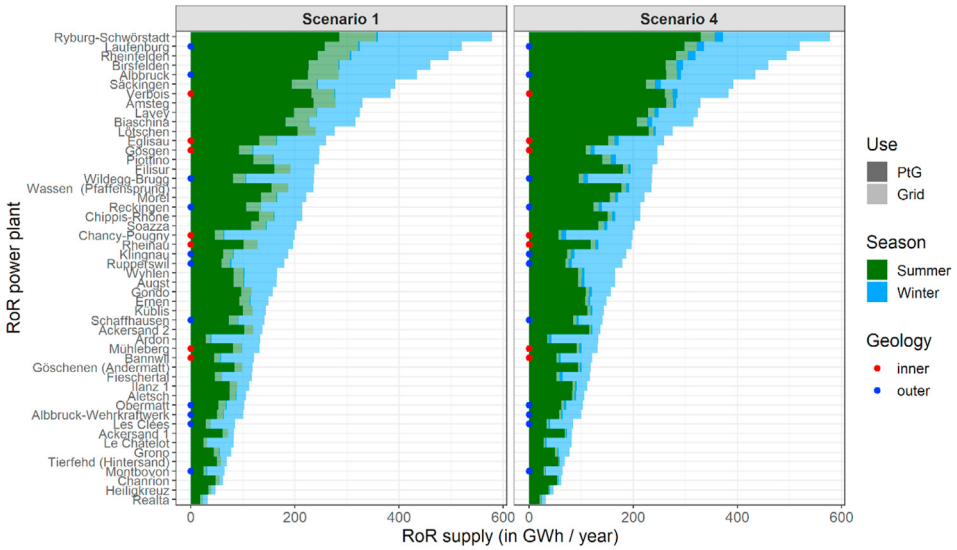

Fig. 9 – Use of electricity for PtG and grid injection in winter (blue) and summer (green) of all RoR power plants larger than 25 MW. The location of each RoR site within the inner (red) and outer (blue) geological perimeter is indicated with coloured dots. Only the results of scenarios 1 and 4 are shown as they are the most distinct. (For interpretation of the references to colour in this figure legend, the reader is referred to the Web version of this article.)

electrification, only about 50% of the available 17–20 TWh net surplus electricity can be simultaneously exploited at these power plants without resorting to additional surplus electricity from the grid at the expense of incurred grid fees. Fig. 8 reveals that the largest amounts of net surplus electricity occur in summer when coincidentally RoR generation is highest, which is a particular reason why situating PtG at RoR power plants is highly suitable in Switzerland [79]. Generation for MWIP is constant throughout the year.

Fig. 9 shows for all RoR power plants (>25 MW_{el}) how much of the generated electricity could be used for PtG and how much electricity is still fed into the electricity grid in each season. RoR power plants within the considered outer and inner geological perimeters are marked by blue and red dots. Only a small portion of the summer generation, irrespective of the size of the RoR power plant, is still fed into the grid. In winter, the situation is reversed and only a small portion is used for PtG as there is almost no net surplus electricity available. Especially for large RoR power plants, their annual electricity generation eligible for PtG may be more than 300 GWh per year (e.g. at RoR power plant Ryburg-Schwörstadt). An analysis of the geological boundary

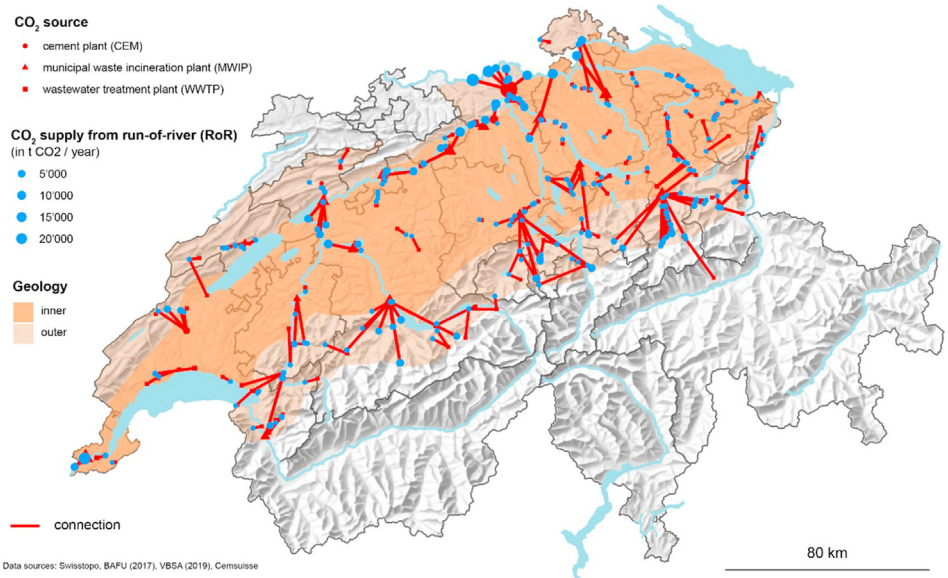

Fig. 10 – Least-cost optimized connections of industrial CO_2 sources and RoR power plants within the inner and outer geologically eligible perimeters for PtG and geo-methanation.

Please cite this article as: Rüdisüli M et al., Potential of renewable surplus electricity for power-to-gas and geo-methanation in Switzerland, International Journal of Hydrogen Energy, https://doi.org/10.1016/j.ijhydene.2022.12.290

conditions (see geological perimeter in Fig. 3) results in a reduction of the exploitable potential to a combined maximum of about 2 TWh in the inner and 4 TWh in the outer perimeter (cf. SI Figs. 6 and 3), compared to the total national potential of about 10 TWh (for scenario 4), if no geological restrictions are considered. More results are provided in SI Section 2.2. Irrespective of the geological perimeter, a small number of RoR power plants could make use of the bulk of the available net surplus electricity.

Transportation distances of CO_2 and gas grid connection

Due to the large amounts of CO_2 emitted by CEM and MWIP, availability of industrial CO_2 is typically never a limiting factor for PtG in the densely populated areas of the Swiss central plateau. The median transportation distance between RoR power plants and CO_2 sites is typically about 4 km. However, for some RoR plants, considerably longer distances of up to 60 km are possible. Distances to the local low-pressure natural gas grid are generally also less than 5 km. However, injection into the high-pressure natural gas grid is typically further away (15–20 km) for both RoR plants and MWIP.

Fig. 10 shows the optimized transportation paths of industrial CO_2 to RoR power plants resulting from the linear transportation problem described in Section 2.5.5. The set of connected CO_2 sources of the largest RoR power plants is shown. Generally, to be cost-optimal, even large RoR power plants feature only one dominant source of CO_2 nearby, which is mostly a MWIP. Only one power plant has two CO_2 sources, namely one WWTP and one MWIP. Additional results of the transportation of CO_2 and the connection to the gas grid are provided in SI Section 2.3.

Ranking of geo-methanation sites

All sites for geo-methanation at RoR plants and MWIP are ranked based on their annual H_2 yield and shown in Table 1 along with their most relevant characteristics. Of the 10 RoR sites with the highest H_2 yield, half are in the outer and inner geological perimeters. Of the 5 top MWIP sites, only Monthey is not in the inner perimeter. The most promising RoR site in the outer perimeter is Laufenburg; in the inner perimeter, it is Verbois. If RoR and MWIP sites are combined, the most suitable MWIP site (Zürich Hagenholz) is only ranked 22. In terms of annual H_2 yield, RoR sites are found to be substantially more productive than MWIP. This is also supported by Gupta et al. [79]. From a geological point of view, the subsurface conditions are most suitable for the sites in the inner geological perimeter situated along the foot of the Jura Mountains and in Northern Switzerland, i.e. along a line Biel – Schaffhausen [34]. The RoR sites along the River Rhine in the outer perimeter (e.g. Laufenburg, Albbruck, Rekingen) are also likely to be suitable in so far as the geological characteristics can be extrapolated into this area with a small degree of uncertainty. In the subsurface at Verbois, Mühlenberg and Zürich Hagenholz the geology is still potentially suitable, but the geological uncertainties in these areas are higher. The geological conditions in Monthey are least suitable for geo-methanation.

However, further evaluation is required based on a full analysis that also accounts for other techno-economic characteristics including CO_2 transportation, equivalent full load hours or natural gas grid injection.

The underground volume available for gas storage in the Swiss Molasse Basin cannot be determined without (a) defining a specific site and geological target formation and (b) detailed investigations of the reservoir formation as the storage volume depends on the theoretical storage capacity multiplied by a storage coefficient. The theoretical storage capacity depends on the volume and connected porosity of the formation as well as the density of the gas mixture at reservoir temperature and pressure. The storage coefficient indicates how much of this capacity can realistically be used, taking into account the irreducible water saturation (i.e., the fraction of porosity filled by formation water that cannot be

Table 1 – Ranking of the top sites for power-to-gas (PtG) and geo-methanation at run-of-river (RoR) and municipal waste incineration plants (MWIP) power plants based on their annual H_2 production via water electrolysis (ELYSE) and other relevant characteristics. Distance is the Euclidian distance (in km) of the CO_2 source, high pressure (HP) and low pressure (LP) gas grid to the PtG site.

#	Power-to-Gas site			Net surplus electricity					H2 prod.		CO2 source					Gas grid	
	Geology perimeter	Power plant	Name	used	used	total gen.	total gen.	eq. FLH	ELYSE	yield	needed	#	Type	Name	Distance	HP	LP
				GWh / year	GWh / summer	GWh / year	GWh / summer	h	MW_el	t H2 / year	t CO2 / year				km	km	km
1	outer	RoR	Laufenburg	320	313	519	323	3427	95	5484	30162	1	CEM	Würenlingen	15	2.1	4.2
2	inner	RoR	Verbois	277	261	384	278	2898	89	4733	26032	1	MWIP	Aire-La-Ville	0	4.2	0.9
3	outer	RoR	Albbruck	274	265	435	284	3425	80	4683	25756	1	CEM	Würenlingen	11	7.0	6.3
4	inner	RoR	Eglisau	163	159	257	165	3150	53	2792	15357	1	MWIP	Dietikon	18	3.1	4.8
5	outer	RoR	Reckingen	132	129	213	133	3509	38	2259	12427	1	CEM	Würenlingen	9	1.6	0.3
6	inner	RoR	Rheinau	126	123	196	127	3523	36	2164	11903	1	MWIP	Winterthur	19	2.8	3.8
7	inner	RoR	Gösgen	108	103	248	107	3247	42	1853	10192	1	MWIP	Oftringen	9	1.2	0.0
8	outer	RoR	Wildegg	94	91	237	95	2567	45	1611	8863	1	CEM	Wildegg	6	4.6	0.6
9	inner	RoR	Mühleberg	93	91	132	97	3106	31	1598	8789	1	MWIP	Bern	10	3.8	5.0
10	outer	RoR	Schaffhausen	90	87	141	91	3571	25	1548	8512	1	MWIP	Winterthur	24	1.5	0.0
22	inner	MWIP	Zürich Hagenh.	55	50	111	56	4368	13	948	5212	1	MWIP	Zürich Hagenh.	0	3.2	0.0
28	inner	MWIP	Zuchwil	49	44	97	49	4368	11	832	4575	1	MWIP	Zuchwil	0	2.1	0.4
30	inner	MWIP	Aire-La-Ville	48	44	96	48	4368	11	818	4500	1	MWIP	Aire-La-Ville	0	3.8	1.1
35	inner	MWIP	Hinwil	40	37	81	40	4368	9	689	3792	1	MWIP	Hinwil	0	2.6	0.1
39	outer	MWIP	Monthey	38	34	75	38	4368	9	643	3539	1	MWIP	Monthey	0	0.3	0.7

Please cite this article as: Rüdisüli M et al., Potential of renewable surplus electricity for power-to-gas and geo-methanation in Switzerland, International Journal of Hydrogen Energy, https://doi.org/10.1016/j.ijhydene.2022.12.290

expelled due to capillary forces upon gas injection) and the proportion of the total pore space in the reservoir that can be reached by injecting gas from a well (whether vertical or horizontal). Storage coefficients have been empirically determined for each of the numerous sedimentary rocks by the oil industry and are typically in the order of 5% [81]. In Austria, where the geological formations of interest for geo-methanation have been identified and well-studied, between 0.5 and 2,900 million m^3 of actual storage volume are discussed [29]. With tentative regard to methane, this would result in a storage capacity of up to about 32 TWh.

Conclusions and outlook

The main contribution of this work is a detailed quantitative assessment of the potential of using power-to-gas for geo-methanation in Switzerland by integrating different modelling approaches. We found that the CO_2 required for geo-methanation is abundantly available in the form of separable industrial CO_2 from cement plants, municipal waste incineration plants and/or wastewater treatment plants. The total available CO_2 would be sufficient to convert 60 TWh of net surplus electricity to CH_4 via power-to-gas and geo-methanation. Thus, CO_2 availability is not a limiting factor for power-to-gas and geo-methanation. Depending on the future Swiss energy system, simulated net surplus electricity ranges between approximately 7 TWh and 20 TWh, corresponding to 10–15% of the total Swiss annual end-use electricity demand. The expected future gas demand (>14 TWh_{th}) is still large enough to use all generated methane from geo-methanation. A re-electrification of this gas in winter is considered to be uneconomical due to additional losses and as enough gas demand remains in energy sectors that are hard to electrify such as industry or heavy-duty transportation.

Only considering RoR power plants in the Swiss Molasse Basin, the total exploitable net surplus electricity in Switzerland is about 2 TWh. By using electricity from RoR sites for PtG, an additional market to sell RoR electricity could be established in times when electricity market prices fall due to PV expansion, reaching potentially even negative electricity prices. Without an additional market for RoR electricity, there is a risk that PV expansion will gradually displace hydropower from the market.

The presented framework allows the most promising sites for using power-to-gas for geo-methanation to be pinpointed, suggesting that MWIP and in particular RoR plants are highly promising sites for PtG. At all Swiss RoR power plants, between 6 and 10 TWh of the total Swiss net surplus electricity could be exploited on-site without resorting to grid electricity and corresponding grid fees. Simulated transportation distances of CO_2 to large RoR power plants are generally below 5 km and the natural gas grid is typically within a short distance from large RoR power plants (<5 km). However, in regions close to the Alps, distances may be longer than 20 km.

The potential cost-benefit of realizing PtG and geo-methanation for Switzerland is challenging due to the estimation of required infrastructure investments, the efficiency of the process as well as changing boundary conditions. Due to the expected impact of exploration and installation costs, a fair economic comparison with conventional catalytic and biological methanation above ground still needs to be established by further research.

The actual storage capacity for geo-methanation in Switzerland must still be refined in further research by more detailed consideration of geological and microbiological boundary conditions as well as more detailed techno-economic assessments of CO_2 transportation, equivalent full load hours or natural gas grid injection. Moreover, as the actual CO_2 feed is non-stoichiometric due to a seasonal mismatch of CO_2 and H_2 supply, the tolerance of geo-methanation for non-stoichiometric feed of CO_2 and H_2 has to be evaluated. If non-stoichiometric feeding of H_2 and CO_2 turns out to be detrimental for geo-methanation, stoichiometric feeding of H_2 and CO_2 with intermediate CO_2 or H_2 storage must be evaluated.

Declaration of competing interest

The authors declare that they have no known competing financial interests or personal relationships that could have appeared to influence the work reported in this paper.

Acknowledgements

This work results from the project “Underground Sun Conversion – Flexible Storage”. The project has been funded by partners of the ERA-Net Smart Energy Systems (eranet-smartenergysystems.eu) and Mission Innovation (mission-innovation.net) through the Joint Call 2019. The authors acknowledge funding from the Swiss Federal Office of Energy under grant agreement SI/502072-01 and European Union's Horizon 2020 research and innovation programme under grant agreements no. 646039 and 775970.

Appendix A. Supplementary data

Supplementary data to this article can be found online at https://doi.org/10.1016/j.ijhydene.2022.12.290.

REFERENCES

[1] BFE. Energieperspektiven 2050+: Technischer Bericht Gesamtdokumentation der Arbeiten. Bern. 2021.
[2] Entso -E. Ten year Network development plan (TYNDP). 2018.
[3] Díaz Redondo P, van Vliet O. Modelling the energy future of Switzerland after the phase out of nuclear power plants. Energy Proc 2015;76:49–58. https://doi.org/10.1016/J.EGYPRO.2015.07.843.
[4] Engeland K, Borga M, Creutin JD, François B, Ramos MH, Vidal JP. Space-time variability of climate variables and intermittent renewable electricity production – a review. Renew Sustain Energy Rev 2017;79:600–17. https://doi.org/10.1016/j.rser.2017.05.046.
[5] Heptonstall PJ, Gross RJK. A systematic review of the costs and impacts of integrating variable renewables into power

grids. Nat Energy 2021;6:72–83. https://doi.org/10.1038/s41560-020-00695-4.
[6] Müller D, Monti A, Stinner S, Schlösser T, Schütz T, Matthes P, et al. Demand side management for city districts. Build Environ 2015;91:283–93. https://doi.org/10.1016/j.buildenv.2015.03.026.
[7] Rüdisüli M, Romano E, Eggimann S, Patel MK. Decarbonization strategies for Switzerland considering embedded greenhouse gas emissions in electricity imports. Energy Pol 2022;162:112794. https://doi.org/10.1016/j.enpol.2022.112794.
[8] Amid A, Mignard D, Wilkinson M. Seasonal storage of hydrogen in a depleted natural gas reservoir. Int J Hydrogen Energy 2016;41:5549–58. https://doi.org/10.1016/j.ijhydene.2016.02.036.
[9] Sun W, Harrison GP, Dodds PE. A multi-model method to assess the value of power-to-gas using excess renewable. Int J Hydrogen Energy 2022;47:9103–14. https://doi.org/10.1016/j.ijhydene.2021.12.248.
[10] Ozturk M, Dincer I. A comprehensive review on power-to-gas with hydrogen options for cleaner applications. Int J Hydrogen Energy 2021;46:31511–22. https://doi.org/10.1016/j.ijhydene.2021.07.066.
[11] Sabatier P, Senderens JB. New methane synthesis. Compte Rendu Acad Sci Paris 1902;134:514–6.
[12] Schneider L, Kötter E. The geographic potential of Power-to-Gas in a German model region-Trier-Amprion 5. J Energy Storage 2015;1:1–6. https://doi.org/10.1016/j.est.2015.03.001.
[13] O'Shea R, Wall DM, McDonagh S, Murphy JD. The potential of power to gas to provide green gas utilising existing CO2 sources from industries, distilleries and wastewater treatment facilities. Renew Energy 2017;114:1090–100. https://doi.org/10.1016/j.renene.2017.07.097.
[14] Guandalini G, Robinius M, Grube T, Campanari S, Stolten D. Long-term power-to-gas potential from wind and solar power: a country analysis for Italy. Int J Hydrogen Energy 2017;42:13389–406. https://doi.org/10.1016/j.ijhydene.2017.03.081.
[15] Reiter G, Lindorfer J. Evaluating CO2 sources for power-to-gas applications-A case study for Austria. J CO2 Util 2015;10:40–9. https://doi.org/10.1016/j.jcou.2015.03.003.
[16] Lisbona P, Frate GF, Bailera M, Desideri U. Power-to-Gas: analysis of potential decarbonization of Spanish electrical system in long-term prospective. Energy 2018;159:656–68. https://doi.org/10.1016/j.energy.2018.06.115.
[17] Bailera M, Lisbona P. Energy storage in Spain: forecasting electricity excess and assessment of power-to-gas potential up to 2050. Energy 2018;143:900–10. https://doi.org/10.1016/j.energy.2017.11.069.
[18] Nielsen S, Skov IR. Investment screening model for spatial deployment of power-to-gas plants on a national scale – a Danish case. Int J Hydrogen Energy 2019;44:9544–57. https://doi.org/10.1016/j.ijhydene.2018.09.129.
[19] Schiebahn S, Grube T, Robinius M, Tietze V, Kumar B, Stolten D. Power to gas: technological overview, systems analysis and economic assessment for a case study in Germany. Int J Hydrogen Energy 2015;40:4285–94. https://doi.org/10.1016/j.ijhydene.2015.01.123.
[20] Heymann F, Rüdisüli M, vom Scheidt F, Camanho AS. Performance benchmarking of power-to-gas plants using Composite Indicators. Int J Hydrogen Energy 2022;47:24465–80. https://doi.org/10.1016/j.ijhydene.2021.10.189.
[21] Teske SL, Rüdisüli M, Schildhauer TJ, Bach C. Potentialanalyse power-to-gas in der Schweiz (potential analysis of power-to-gas in Switzerland). Dübendorf: Empa 2021. https://doi.org/10.5281/zenodo.2649817.
[22] Kober T, Bauer (eds) C, Bach C, Beuse M, Georges G, Held M, et al. White paper "power-to-X: perspectives in Switzerland. Villigen; 2019.
[23] Nazir H, Muthuswamy N, Louis C, Jose S, Prakash J, Buan MEM, et al. Is the H2 economy realizable in the foreseeable future? Part III: H2 usage technologies, applications, and challenges and opportunities. Int J Hydrogen Energy 2020;45:28217–39. https://doi.org/10.1016/j.ijhydene.2020.07.256.
[24] Mitteregger M, Bauer S, Loibner AP, Schritter J, Gubik A, Backes D, et al. Method for the hydrogenotrophic methanogenesis of H2 and CO2 into CH4. WO 2016/151078 Al. 2015.
[25] Götz M, Lefebvre J, Mörs F, McDaniel Koch A, Graf F, Bajohr S, et al. Renewable Power-to-Gas: a technological and economic review. Renew Energy 2016;85:1371–90. https://doi.org/10.1016/j.renene.2015.07.066.
[26] Strobel G, Hagemann B, Huppertz TM, Ganzer L. Underground bio-methanation: concept and potential. Renew Sustain Energy Rev 2020;123:109747. https://doi.org/10.1016/j.rser.2020.109747.
[27] Pichler M, Bauer S, Loibner A, Konegger H, Zanghellini J, Trautmann A, Mori G, Makaruk A, Wintersperger J, et al. Underground Sun Conversion, Renewable energy storage and conversion by in-situ biological methanation in porous Underground gas reservoirs. Vienna: Report Climate and Energy Fund; 2021.
[28] Dopffel N, Jansen S, Gerritse J. Microbial side effects of underground hydrogen storage – knowledge gaps, risks and opportunities for successful implementation. Int J Hydrogen Energy 2021;46:8594–606. https://doi.org/10.1016/j.ijhydene.2020.12.058.
[29] RAG. Unterground Sun conversion. 2021.
[30] Zivar D, Kumar S, Foroozesh J. Underground hydrogen storage: a comprehensive review. Int J Hydrogen Energy 2021;46:23436–62. https://doi.org/10.1016/j.ijhydene.2020.08.138.
[31] RAG. Unterground Sun Storage. 2017.
[32] Koirala B, Hers S, Morales-España G, Özdemir Ö, Sijm J, Weeda M. Integrated electricity, hydrogen and methane system modelling framework: application to the Dutch Infrastructure Outlook 2050. Appl Energy 2021;289. https://doi.org/10.1016/j.apenergy.2021.116713.
[33] Eggimann S, Hall JW, Eyre N. A high-resolution spatio-temporal energy demand simulation to explore the potential of heating demand side management with large-scale heat pump diffusion. Appl Energy 2019;236:997–1010. https://doi.org/10.1016/j.apenergy.2018.12.052.
[34] van den Heuvel DB, Diamond LW, Musso Piantelli F, Garefalakis P. Geological suitability of the Swiss Molasse Basin for gas storage and geo-methanation: a literature study. University of Bern, Switzerland: Bern; 2022.
[35] Kober T, Bauer C, Bach C, Beuse M, Georges G, Held M, et al. Perspectives of power-to-X technologies in Switzerland. A White Paper 2019. https://doi.org/10.3929/ethz-b-00035229.
[36] Rüdisüli M, Teske SL, Elber U. Impacts of an increased substitution of fossil energy carriers with electricity-based technologies on the Swiss electricity system. https://doi.org/10.20944/PREPRINTS201905.0179.V1; 2019.
[37] Swisstopo GeoMol. A geological 3D model of the Swiss Plateau. Swiss Federal Office of Topography, Wabern. 2021.
[38] KSDL-OCAR. Koordinationsstelle Durchleitung. 2021.
[39] Chevalier G, Diamond LW, Leu W. Potential for deep geological sequestration of CO2 in Switzerland: a first appraisal. Swiss J Geosci 2010;103:427–55. https://doi.org/10.1007/s00015-010-0030-4.

Please cite this article as: Rüdisüli M et al., Potential of renewable surplus electricity for power-to-gas and geo-methanation in Switzerland, International Journal of Hydrogen Energy, https://doi.org/10.1016/j.ijhydene.2022.12.290

[40] Allenbach R, Baumberger R, Kurmann E, Michael CS, Reynolds L. GeoMol: geologisches 3D-Modell des Schweizer Molassebeckens – Schlussbericht. Swiss Federal Office of Topography, Wabern; 2017.
[41] Mutschler R, Rüdisüli M, Heer P, Eggimann S. Benchmarking cooling and heating energy demands considering climate change, population growth and cooling device uptake. Appl Energy 2021;288:116636. https://doi.org/10.1016/j.apenergy.2021.116636.
[42] BFE. Analyse des schweizerischen Energieverbrauchs 2000-2018 – Auswertung nach Verwendungszwecken (Analysis of Swiss energy consumption 2000-2018 - evaluation according to purpose). Bern: Bundesamt für Energie BFE (Swiss Federal Office of Energy (SFOE); 2019.
[43] VSG. Erdgas und Biogas in der Schweiz - jahresstatistik des VSG. gaz energie; 2020.
[44] BFE. Schweizerische elektrizitätsstatistik (Swiss electricity statistics). 2017. p. 2017.
[45] Swissgrid. Aggregierte Energiedaten aus dem Regelblock Schweiz (Aggregated energy data from the Swiss control block). https://www.swissgrid.ch/de/home/customers/topics/energy-data-ch.html. [Accessed 24 November 2020].
[46] Hirth L, Mühlenpfordt J, Bulkeley M. The ENTSO-E Transparency Platform – a review of Europe's most ambitious electricity data platform. Appl Energy 2018;225:1054–67. https://doi.org/10.1016/j.apenergy.2018.04.048.
[47] BFE, Schweizerische. Statistik der erneuerbaren Energien (Swiss statistics on renewable energies). 2019. p. 2019.
[48] Pfenninger S, Staffell I. Long-term patterns of European PV output using 30 years of validated hourly reanalysis and satellite data. Energy 2016;114:1251–65. https://doi.org/10.1016/j.energy.2016.08.060.
[49] Walch A, Castello R, Mohajeri N, Scartezzini J-L. Big data mining for the estimation of hourly rooftop photovoltaic potential and its uncertainty. Appl Energy 2020;262:114404. https://doi.org/10.1016/j.apenergy.2019.114404.
[50] MeteoSwiss. IDAWEB 2020.
[51] Walch A, Rüdisüli M. Strategic PV expansion and its impact on regional electricity self-suffciency: case study of Switzerland. Appl Energy 2022 [submitted] for publication.
[52] BFE, Schweizerische. Elektrizitätsstatistik (Swiss electricity statistics). 2016. p. 2016.
[53] Swiss Federal Office of Energy. Statistics on hydropower plants (WASTA). 2021.
[54] Von Roon S, Huber M. Modeling spot market pricing with the residual load, Munich: enerday - 5th conference on energy economics and technology. Dresden; 2010. 16.04.2010.
[55] Dillig M, Jung M, Karl J. The impact of renewables on electricity prices in Germany - an estimation based on historic spot prices in the years 2011-2013. Renew Sustain Energy Rev 2016;57:7–15. https://doi.org/10.1016/j.rser.2015.12.003.
[56] Beer M. Abschätzung des Potenzials der Schweizer Speicherseen zur Lastdeckung bei Importrestriktionen (Assessment of the potential of Swiss storage lakes to cover loads in the event of import restrictions). Z Energiewirtschaft 2018;42:1–12. https://doi.org/10.1007/s12398-018-0220-8.
[57] Piot M. Bedeutung der Speicher-und Pumpspeicherkraftwerke für die Energiestrategie 2050 der Schweiz (Significance of storage and pumped storage power plants for Switzerland's 2050 energy strategy). Wasser, Energ Luft 2014;4:259–65.
[58] Swissmem. Energie- und CO2-Statistik. 2017.
[59] BAFU, Schadstoffregister. SwissPRTR (pollutant register SwissPRTR). 2019.
[60] Wurzbacher J. Capturing CO2 from air. In: L J, B C, editors. Int. Mot. Wiesbaden: Springer Vieweg; 2017. p. 499–511. https://doi.org/10.1007/978-3-658-17109-4_32.
[61] Beuttler C, Charles L, Wurzbacher J. The role of direct air capture in mitigation of anthropogenic greenhouse gas emissions. Front Clim 2019;1:10. https://doi.org/10.3389/fclim.2019.00010.
[62] Schweizer Zement. Berichterstattung cemsuisse. 2018.
[63] Volkart K, Bauer C, Boulet C. Life cycle assessment of carbon capture and storage in power generation and industry in Europe. Int J Greenh Gas Control 2013;16:91–106. https://doi.org/10.1016/J.IJGGC.2013.03.003.
[64] Meier B, Ruoss F, Friedl M. Investigation of carbon flows in Switzerland with the special consideration of carbon dioxide as a feedstock for sustainable energy carriers. Energy Technol 2017;5:864–76. https://doi.org/10.1002/ente.201600554.
[65] INFRAS. Emissionsfaktoren für stationäre Quellen. Berm; 2000.
[66] VBSA. Kehricht-verwertungs-anlagen (KVA). 2019.
[67] VBSA. Monitoring-Bericht zur CO2-Branchenvereinbarung für das Jahr 2015 (Monitoring report on the 2015 CO2 interbranch agreement). Bern: bundesamt für Umwelt BAFU (Federal Office for the Environment FOEN)/Bundesamt für Energie BFE. Swiss Federal Office of Energy SFOE); 2016.
[68] Federal Office for the Environment. Indicators waste 2021.
[69] Johnke B. Emissions from waste incineration. In: Penman J, Kruger D, Galbally I, Hiraishi T, Nyenzy B, Emmanul S, et al., editors. Good pract. Guid. Uncertain. Manag. Natl. Greenh. Gas invent. Montreal: Intergovernmental Panel on Climate Change (IPCC); 2001. p. 455–68.
[70] Reinhardt T, Richers U, Suchomel H. Hazardous waste incineration in context with carbon dioxide. Waste Manag Res 2008;26:88–95. https://doi.org/10.1177/0734242X07082339.
[71] BAFU, Faktenblatt. CO2 Emissionsfaktoren des Treibhausgasinventars der Schweiz (Fact sheet: CO2 Emission factors of the greenhouse gas inventory of Switzerland). 2015.
[72] Gujer W. Siedlungswasserwirtschaft. Springer; 1999.
[73] Peyer T, Nijsen R, Heller T, Reuter M. Kläranlagen - ideal für Power-to-Gas. Aqua Gas 2016;7/8:42–6.
[74] Witte J, Settino J, Biollaz SMA, Schildhauer TJ. Direct catalytic methanation of biogas – Part I: new insights into biomethane production using rate-based modelling and detailed process analysis. Energy Convers Manag 2018;171:750–68. https://doi.org/10.1016/J.ENCONMAN.2018.05.056.
[75] BAFU. Adressliste der Schweizer Kläranlagen mit Angaben zur Ausbaugrösse (Address list of the Swiss sewage treatment plants with information on the expansion size). 2017.
[76] AFU. ARA. Steckbriefe (fact sheets WWTP). 2019.
[77] Berkelaar M. Package ' lpSolve '. 2020.
[78] Lienhard N, Mutschler R, Ludger L, Rüdisüli M. Concurrent deficit -and surplus situations in the future renewable Swiss and European electricity system energy strategy reviews. Energy Strateg Rev 2022 [accepted] for publication.
[79] Gupta R, Rüdisüli M, Patel MK, Parra D. Smart power-to-gas deployment strategies informed by spatially explicit cost and value models. Appl Energy 2022;327:120015. https://doi.org/10.1016/j.apenergy.2022.120015.
[80] Gupta R, Pena-Bello A, Streicher KN, Roduner C, Farhat Y, Thöni D, et al. Spatial analysis of distribution grid capacity and costs to enable massive deployment of PV, electric mobility and electric heating. Appl Energy 2021;287:116504. https://doi.org/10.1016/j.apenergy.2021.116504.
[81] Gorecki CD, Sorensen JA, Bremer JM, Knudsen DJ, Smith SA, Steadman EN, et al. Development of storage coefficients for determining the effective CO2 storage resource in deep saline formations. All days. SPE; 2009. https://doi.org/10.2118/126444-MS.

Please cite this article as: Rüdisüli M et al., Potential of renewable surplus electricity for power-to-gas and geo-methanation in Switzerland, International Journal of Hydrogen Energy, https://doi.org/10.1016/j.ijhydene.2022.12.290